

High Speed Visible Light Communication Using Digital Power Domain Multiplexing of Orthogonal Frequency Division Multiplexed (OFDM) Signals

Wahyu-Hendra Gunawan ¹, Yang Liu ², Chi-Wai Chow ^{1,*}, Yun-Han Chang ¹ and Chien-Hung Yeh ³

¹ Department of Photonics, College of Electrical and Computer Engineering, National Yang Ming Chiao Tung University, Hsinchu 30010, Taiwan; wahyuhendrag.eo07g@nctu.edu.tw (W.-H.G.); yhchang.eo08g@nctu.edu.tw (Y.-H.C.)

² Philips Electronics Ltd., N.T., Hong Kong; yang.y.liu@lumileds.com

³ Department of Photonics, Feng Chia University, Taichung 40724, Taiwan; yehch@fcu.edu.tw

* Correspondence: cwchow@faculty.nctu.edu.tw

Abstract: In order to increase transmission capacity, multiplexing schemes in different physical dimensions, including time, frequency, modulation quadrature, polarization, and space, can be employed. In this work, we propose and demonstrate a red color laser-diode (LD) based visible-light-communication (VLC) system using two kinds of digital domain multiplexing schemes, orthogonal-frequency-division-multiplexing (OFDM) and power-domain division-multiplexing (PowDM). The two digital domain multiplexed data can achieve data rates of 1.66 Gbit/s and 6.41 Gbit/s, respectively, providing a total data rate of 8.07 Gbit/s, fulfilling the pre-forward error correction (pre-FEC) bit-error-rate (BER) limit. The measured signal-to-noise ratios (SNRs) are 10.96 dB and 14.45 dB, respectively. Here, similar to OFDM, the PowDM can enhance the total system capacity by allowing acceptable signal spectra overlapping among different power division signals to maximize the bandwidth utilization. An experiment to verify and evaluate the proposed work is performed. The modulation and demodulation of OFDM and PowDM are discussed. The optimum power levels of the individual signals in the PowDM signal are also analyzed.

Keywords: optical wireless communication (OWC); visible light communication (VLC); orthogonal frequency division multiplexing (OFDM); laser diode (LD)



Citation: Gunawan, W.-H.; Liu, Y.; Chow, C.-W.; Chang, Y.-H.; Yeh, C.-H. High Speed Visible Light Communication Using Digital Power Domain Multiplexing of Orthogonal Frequency Division Multiplexed (OFDM) Signals. *Photonics* **2021**, *8*, 500. <https://doi.org/10.3390/photonics8110500>

Received: 26 September 2021

Accepted: 2 November 2021

Published: 8 November 2021

Publisher's Note: MDPI stays neutral with regard to jurisdictional claims in published maps and institutional affiliations.



Copyright: © 2021 by the authors. Licensee MDPI, Basel, Switzerland. This article is an open access article distributed under the terms and conditions of the Creative Commons Attribution (CC BY) license (<https://creativecommons.org/licenses/by/4.0/>).

1. Introduction

Visible light communication (VLC) is an attractive and promising technology for future wireless communication systems [1]. VLC is a kind of optical wireless communication (OWC) using visible light spectrum for communication. Due to the advances of light emitting diode (LED) development, VLC systems can be based on existing lighting infrastructure to provide illumination and communication at the same time [2]. Due to the highly directional feature of the optical light beam, VLC could provide highly directional and high privacy transmission, at the same time being immune to radio-frequency (RF) electromagnetic interference (EMI) [3]. Different VLC technologies have been studied in ref. [4]. Due to the many unique advantages offered by VLC, it has been considered as one of the potential candidates for beyond 5G or 6G mobile and wireless communication [5]. There are many potential applications of VLC systems, such as vehicle to vehicle communication [6], visible light positioning (VLP) [7], robot navigation in hospitals [8], underwater communication [9], optical camera communication (OCC) [10], display and sign board communication [11].

One popular VLC transmitter (Tx) is the LED [12]. A phosphor-based LED Tx for both lighting and VLC has been reported [13]. As the data rate of the LED based VLC system is limited by the relaxation time of the yellow phosphor, schemes include pre/post-equalization [14], multiple-input multiple-output (MIMO) [15], etc. Hsu et al. reported

a 1.1 Gbit/s white-light VLC system based on 3×3 MIMO [15]. Cossu et al. reported a 3.4 Gbit/s VLC system based on wavelength division multiplexing of red green blue (RGB) LEDs [16]. Besides, Chi et al. also reported a 3.375 Gbit/s RGB LEDs based WDM VLC system using high level modulation (i.e., eight levels of pulse amplitude modulation, PAM 8) [17]. To further enhance the modulation bandwidth, micro-LEDs can also be employed [18]. Tsonev et al. reported a 3 Gbit/s VLC link using a blue gallium nitride (GaN) micro-LED and high spectral efficient orthogonal frequency division multiplexing (OFDM) format [19]. Recently, Lan et al. reported a 1 Gbit/s on-off-keying (OOK) VLC system using a violet micro-LED [20]. By growing the micro-LED in non-polar or semi-polar orientations, the quantum confined stark effect (QCSE) can be reduced and a higher modulation bandwidth can be achieved. Chang et al. reported a 4.343 Gbit/s VLC transmission based on a green semipolar micro-LED array [21]. To suppress the LED efficiency droop [22] and enhance the modulation bandwidth, the laser diode (LD) can also be a promising candidate for VLC. LD based VLC is one of the best choices for high-speed data transmission, such as simultaneous lighting and communication [23], machine to machine communication [24], underwater communication [25], and mobile back-haul transmission [26]. Wei et al. demonstrated a 6.915 Gbit/s white-light illumination and VLC system using blue LD with yellow phosphor [27] and these can be used for illumination and communication simultaneously. In order to further increase the transmission capacity, multiplexing schemes in different physical dimensions, including time, frequency, modulation quadrature, polarization, and space, can be employed. Wu et al. reported a VLC system using WDM RGB LDs operated at 8 Gbit/s [28] and Wei et al. illustrated a LD based VLC system combining WDM and polarization division multiplexing (PolDM) which operated at 40.665 Gbit/s [29]. Moreover, Gunawan et al. also illustrated an LD based VLC system for color-shift-keying (CSK) [30]. Besides the physical domain multiplexing schemes, digital domain multiplexing schemes such as OFDM [31] can also enhance the total system capacity by allowing a certain degree of signal spectral overlapping to maximize the bandwidth utilization. The OFDM system divides the data signal into several lower bit rate subcarriers, which are orthogonal to each other. By employing fast-Fourier transform (FFT) at the receiver (Rx) side, the data signal can be retrieved even if there is strong spectral overlapping among the OFDM subcarriers. Hence, a high spectral efficiency can be achieved.

In this work, we put forward and experimentally demonstrate an 8.07 Gbit/s red color LD based VLC system using two kinds of digital domain multiplexing schemes, OFDM and power domain division multiplexing (PowDM). The PowDM technique is inspired by the works [32,33], where [32] is related to power domain multiplexing for multiple users and [33] is applied for a fiber coherent transmission system. Here, similar to OFDM, the PowDM can also enhance the total system capacity by allowing acceptable signal spectra overlapping among different power division signals to maximize the bandwidth utilization. By employing the successive interference cancellation (SIC) at the Rx side, the data signal can be retrieved. The potential applications of the proposed method can be used in machine-to-machine communication (M2M) or in areas where the employment of RF based wireless communication is forbidden. An experiment to verify and evaluate the proposed work is performed, and the results show that the PowDM signal can achieve a higher capacity than the individual signal. The modulation and demodulation of the OFDM and PowDM are discussed. The optimum power levels of the individual signals in the PowDM signal are also analyzed.

2. Principle and Experiment

Here, the principle of the PowDM will be presented. Without loss of generality, we illustrate the principle of PowDM by assuming that the data are divided into two individual signals, x_i , where $i = 1$ and 2. The corresponding transmission powers are P_i , where $i = 1$

and 2. In the system, there is a single LD at the Tx and a single photodiode (PD) at the Rx. The sum of total power P_i is equal to P . The transmitted signal is shown in Equation (1).

$$x = \sqrt{P_1}x_1 + \sqrt{P_2}x_2 \quad (1)$$

The received signal can be illustrated in Equation (2),

$$y_i = h_i x + n_i \quad (2)$$

where h_i is the channel response between the Tx and Rx, and the n_i represents the noises. According to Equation (1), different individual signals in the PowDM signal should maintain a certain power ratio for the successful decoding of individual signals, Data 1 and Data 2 at the Rx. At the Rx, the SIC process is performed and the decoding priority is based on the order of the increasing channel gain. With the example of 2 individual signals with $P_2 > P_1$, x_2 signal will be recovered first without the need of SIC since it has a higher power than x_1 . Then, the decoded x_2 will be used to retrieve x_1 in the SIC process [32] by subtracting itself from the received signal.

Based on the Shannon–Hartley equation, the channel capacity C is related to the theoretical limit of the information data rate, which is equal to the channel bandwidth B times the logarithm of one plus the signal-to-noise ratio (SNR). Hence, the total capacity of the PowDM signal can be written in Equation (3).

$$\begin{aligned} C &= C_2 + C_1 \\ &= B \log_2 \left(1 + \frac{|h_2|^2 P_2}{|h_1|^2 P_1 + P_N} \right) + B \log_2 \left(1 + \frac{|h_1|^2 P_1}{P_N} \right) \end{aligned} \quad (3)$$

As shown in Equation (3), the total channel capacity C is equal to the capacities of the two individual signals C_2 and C_1 . The channel responses of individual Data 2 and Data 1 are h_2 and h_1 respectively. Since there is only one Tx and one Rx, the Data 2 and Data 1 share the same bandwidth B and noise power P_N . It is worth noting that for Data 2, the capacity C_2 is affected by the transmission noise P_N plus the interference from the Data 1 (P_1) during the PowDM. For Data 1, the capacity C_1 is affected by P_N only. However, a certain ratio of P_2 to P_1 should be maintained in PowDM, and the power level of P_1 is limited. This will also affect the capacity C_1 . In this proof-of-concept demonstration, only 2 power-division channels are used. More channels can be supported if the SNR of the transmitted signal is high enough [34].

Figure 1 shows the principle of encoding and decoding of the proposed PowDM VLC system. At the Tx side, two individual data signals (Data 1 and Data 2) are first mapped to quadrature phase shift keying (QPSK) formats. Then the signals are allocated to subcarriers according to channel conditions. After this, the two signals at different power levels are combined with superposition code (SC) [32], which realizes multiplexing in the power domain. Hence the constellation diagrams are shaped according to the power allocation. This can be implemented by multiplying the signals by specified power levels P_1 or P_2 . Inverse fast Fourier transformation (IFFT) is used to convert the signal from the frequency domain into time domain. Hermitian symmetry is utilized to produce real-valued OFDM signal for driving the LD. After this, parallel-to-serial (P/S) conversion and the addition of a cyclic prefix (CP) are performed. After the PowDM OFDM signal is generated, it is applied to a LD via a digital-to-analog converter (DAC). The signal will then be received by a PD via an optical channel. The received PowDM OFDM signal will be converted into a digital signal via an analog-to-digital converter (ADC). Synchronization schemes are applied. After this, serial-to-parallel (S/P) conversion is performed to retrieve the information in subcarriers. Zero-forcing scheme is used to restore the signal after the channel, and fast Fourier transform (FFT) is used to convert it into the frequency domain. In the PowDM decoding, Data 2 can be decoded first while considering Data 1 as noise, so direct QPSK demodulation can be applied. Then, SIC is employed to subtract the retrieved

Data 2 from the main signal before the QAM demodulation applied. After this, FFT and QPSK demodulation are executed to retrieve the Data 1.

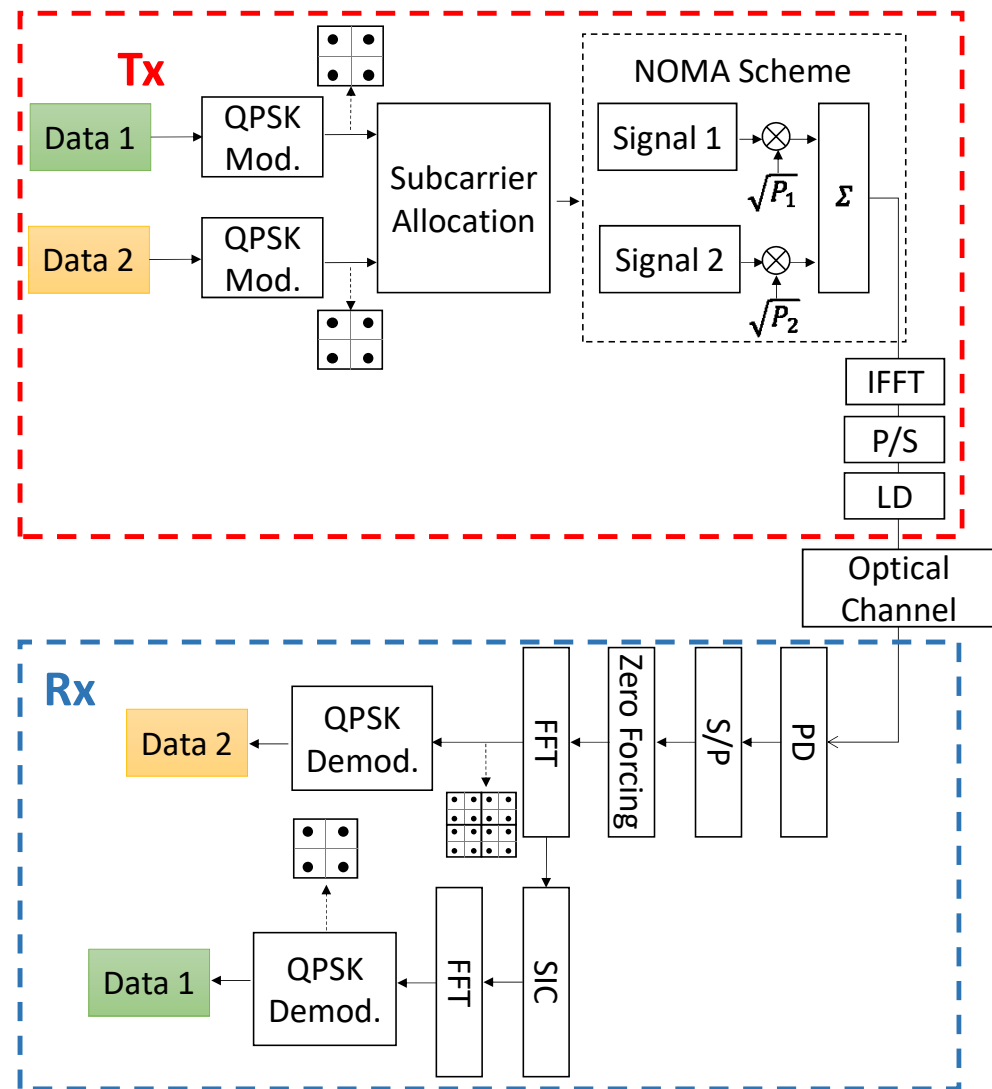


Figure 1. Principle of encoding and decoding of the proposed PowDM VLC system. QPSK: quadrature phase shift keying; IFFT: inverse fast Fourier transformation; P/S: parallel-to-serial; LD: laser diode; PD: photodiode; S/P: serial-to-parallel; SIC: successive Interference cancellation.

Figure 2 illustrates the experiment of the proposed PowDM VLC system. A photo of the experimental setup is shown in inset of Figure 2. As discussed in pervious paragraphs, Data 1 and Data 2 with proper power ratio are combined in the digital domain using off-line program. Then, the PowDM data stored in an arbitrary waveform generator (AWG, Tektronix® AWG 70001) act as the DAC converting the PowDM digital data into real electrical waveform to drive a LD. The AWG has the sampling rate of 50 GSample/s and resolution of 8 bits. It has an analog frequency range of 18 GHz. Then, the PowDM electrical signal is used to drive a red LD via a bias-tee circuit. The red LD (Opnext® HL6544FM) used has a peak wavelength of 640 nm. It is based on AlGaInP with multi-quantum well (MQW) structure. After a free-space transmission distance of 1.5 m, the optical signal is detected by a PIN PD (EOT ET-2030A). After the optical signal has propagated 1.5 m transmission distance, the optical beam diameter at the Rx is 4 mm. It is silicon-based with a bandwidth of 1.2 GHz. The active area diameter and the acceptance full angle are 400 µm and 20°, respectively. The PD is attached to a real-time oscilloscope (RTO, Teledyne LeCroy® 816ZI-B) acting as the ADC converting the received waveform into digital data for

signal processing. The RTO has the sampling rate of 80 GSample/s and analog bandwidth of 16 GHz. In the experiment, the FFT size 512, number of subcarriers is 125, and CP is 32. Table 1 summarizes all the system parameters.

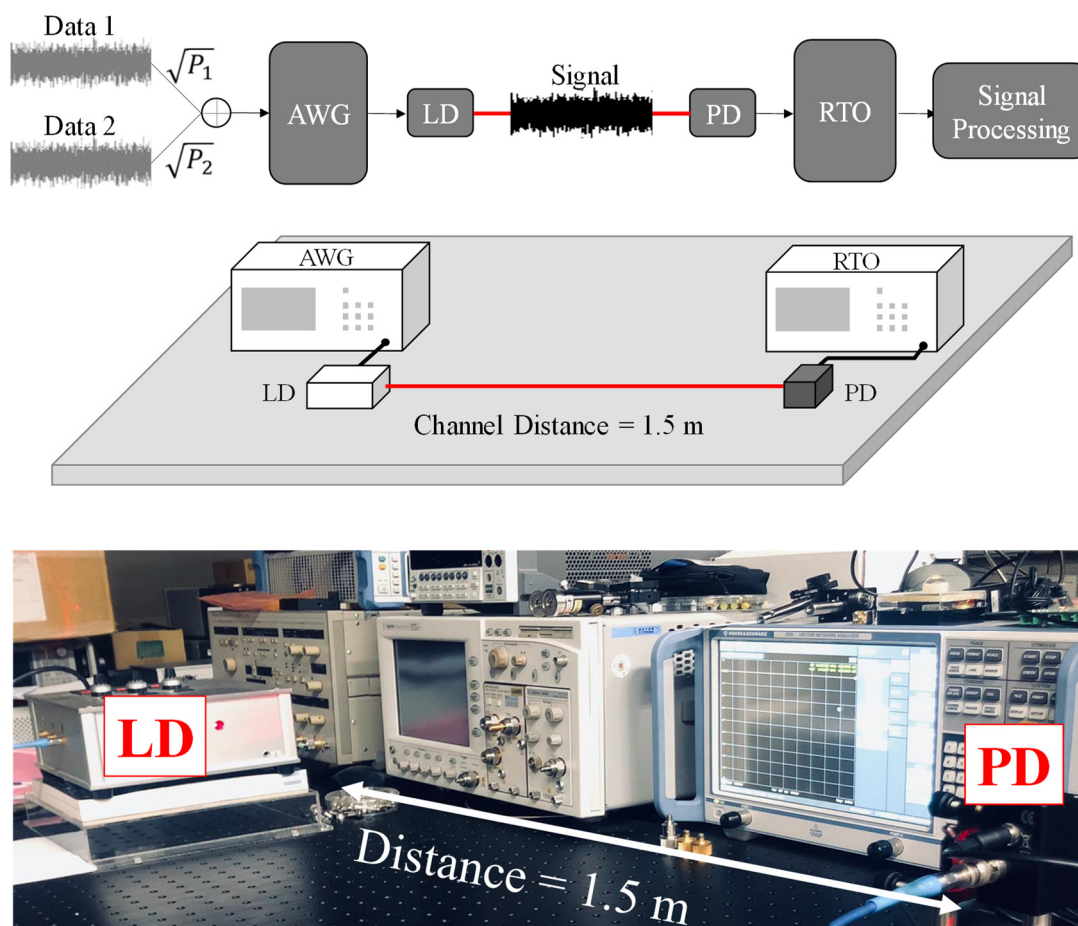


Figure 2. Experiment of the proposed PowDM VLC system. AWG: arbitrary waveform generator; RTO: real-time oscilloscope. Inset: a photo of the experimental setup.

Table 1. System Parameters.

System Parameter		
FFT Size		512
Subcarrier		125
Cyclic Prefix		32
LD Drive Current		70 mA
AWG Bandwidth		18 GHz
PD Bandwidth		1.2 GHz
RTO Bandwidth		16 GHz
Transmission Distance		1.5 m

3. Results and Discussion

In the experiment, a commercially available red LD is employed. It is based on AlGaInP with a multi-quantum well (MQW) structure. It has a maximum optical output power of about 130 mW. Figure 3 shows the measured characteristics of the red LD. The threshold currents is about 60 mA. The inset in Figure 3 shows the measured optical spectrum and the peak emission wavelength is 640 nm.

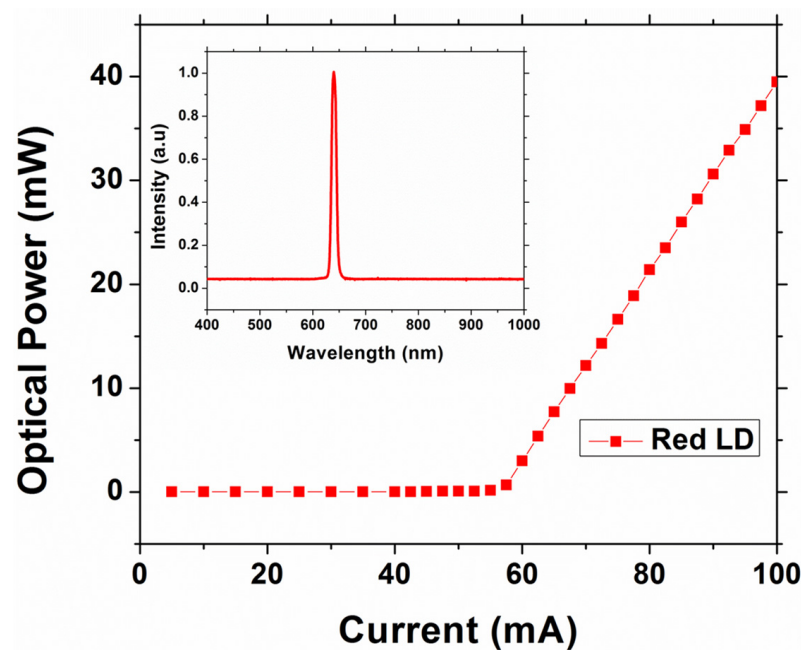


Figure 3. Measured characteristics of the red LD used in the experiment. Inset: measured optical spectrum.

As the two individual data signals are superimposed in the power domain and the constellation diagrams are shaped according to the power allocation, it is important to obtain the optimum power ratio to maximize the system throughput and to minimize the bit error ratio (BER) of both data. To simplify the DSP of Tx and Rx, the power ratio is applied to all the subcarriers. Figure 4 shows measured BER against power ratio of Data 2 to Data 1 of the PowDM VLC system. The power ratio has a significant effect on Data 1 since it will highly affect the shape of the constellation diagram of the main signal, introducing high error during the implementation of the SIC. We can also observe that the power ratio only has a small effect on the Data 2. This is because the demodulation of the 16-quadrature amplitude modulation (QAM) like signal is divided into four quadrants, and the constellation points in each quadrant will be mapped to the same Data 2 logic bit. The constellation diagrams of Data 1 and Data 2 are also illustrated in Figure 4. In the experiment, when the power ratios are larger than 5 dB, the BER performances of Data 1 and Data 2 are 2.41×10^{-3} and 3.94×10^{-3} . Both data can satisfy the 7% pre-forward-error-correction (pre-FEC) BER of 3.8×10^{-3} .

Figure 5 shows the measured BER curves of the two individual signals and the PowDM signal at different data rate. By considering the FEC limit, Data 1 can achieve a data rate of 1.66 Gbit/s at BER of 2.20×10^{-3} and Data 2 can achieve a data rate of 6.41 at BER of 1.21×10^{-3} . Hence, the maximum data rate achieved by the PowDM signal fulfilling the pre-FEC BER limit is 8.07 Gbit/s at the BER of 1.7×10^{-3} .

Finally, the SNRs of the Data 1 and Data 2 in the proposed PowDM signal are also evaluated. Figure 6 shows the measured SNRs of the two individual signals against all the OFDM subcarriers in the proposed PowDM VLC system. The average SNR for Data 1 is 10.96 dB and the average SNR for Data 2 is 14.45 dB. The corresponding achieved data rates for Data 1 and Data 2 are 1.66 Gbit/s and 6.41 Gbit/s, respectively.

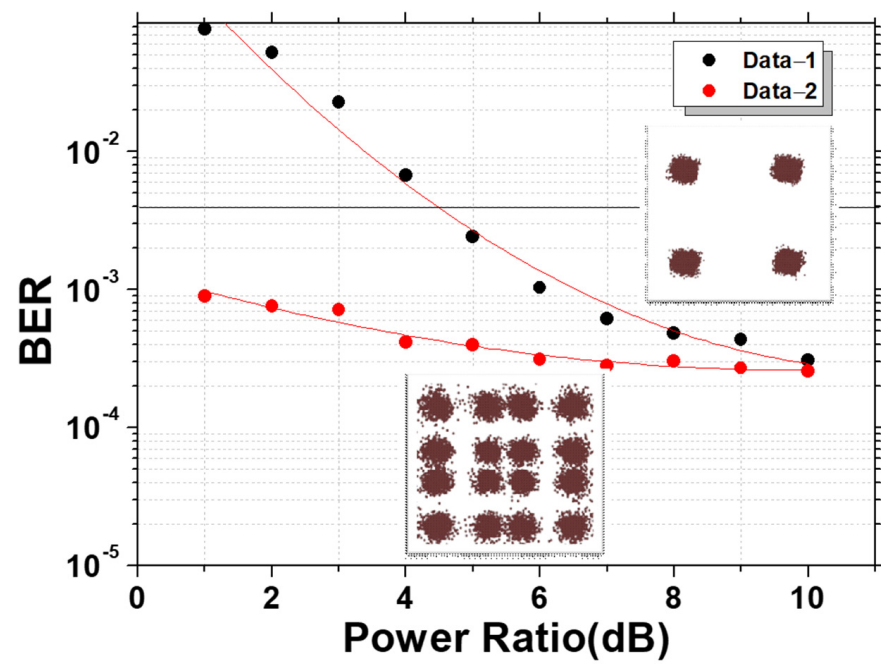


Figure 4. Measured BER against power ratio of Data 2 to Data 1 of the PowDM VLC system. Insets: constellation diagrams of Data 1 and Data 2.

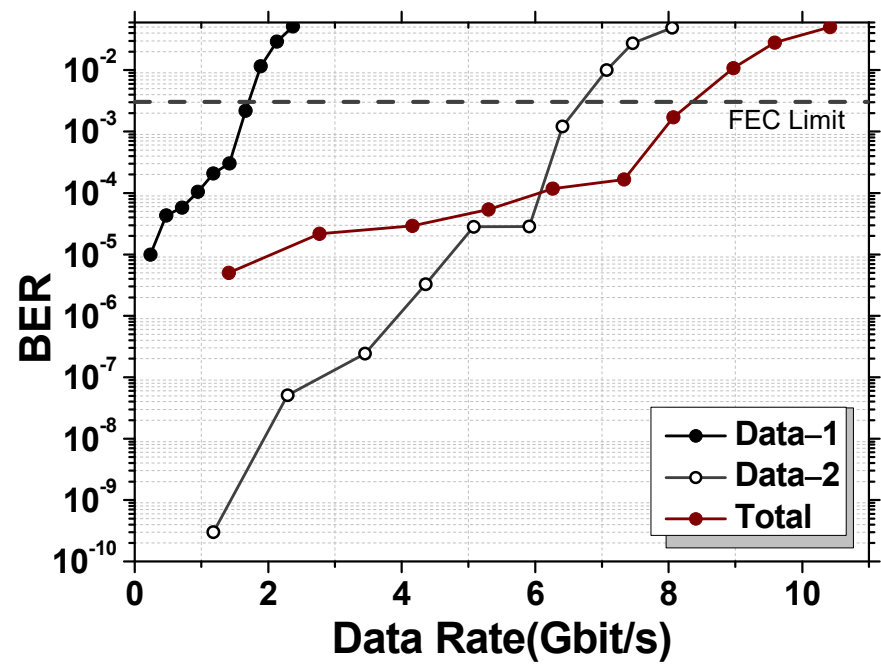


Figure 5. Measured BER curves of the two individual signals and the PowDM signal.

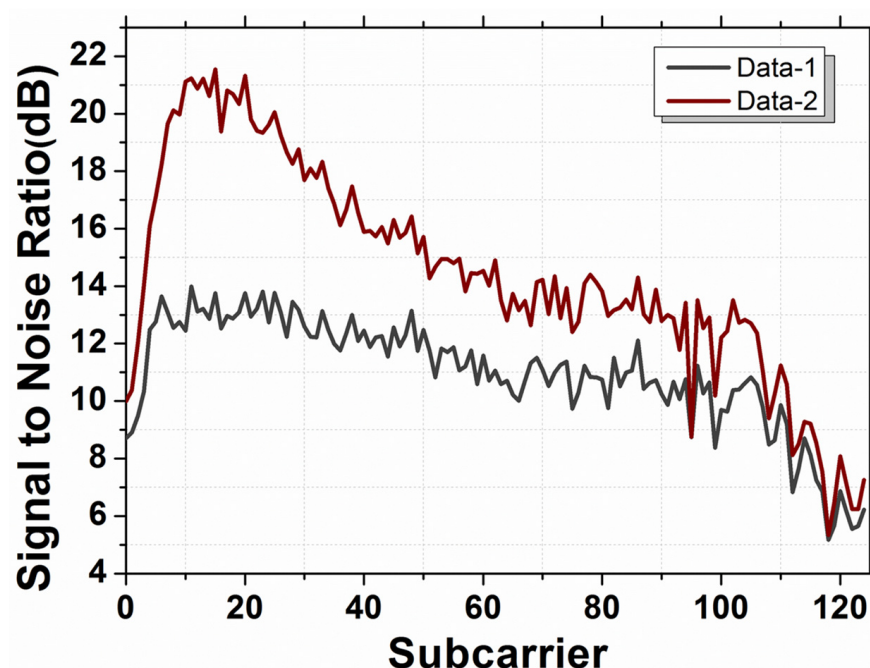


Figure 6. Measured SNRs of the two individual signals against all the OFDM subcarriers in the proposed PowDM VLC system.

4. Conclusions

In this work, we proposed and demonstrated an 8.07 Gbit/s red color LD based VLC system using two kinds of digital domain multiplexing schemes, OFDM and PowDM. Here, similar to OFDM, the PowDM can also enhance the total system capacity by allowing acceptable signal spectra overlapping among different power division signals to maximize the bandwidth utilization. By employing the SIC at the Rx side, the data signal can be retrieved. The modulation and demodulation of the OFDM and PowDM are discussed. In the experiment, when the power ratios are larger than 5 dB, the BER performances of Data 1 and Data 2 are 2.41×10^{-3} and 3.94×10^{-3} . Both data can satisfy the 7% pre-forward-error-correction (pre-FEC) BER of 3.8×10^{-3} . By considering the FEC limit, Data 1 can achieve a data rate of 1.66 Gbit/s at BER of 2.20×10^{-3} and Data 2 can achieve a data rate of 6.41 Gbit/s at BER of 1.21×10^{-3} . Hence, the maximum data rate achieved by the PowDM signal fulfilling the pre-FEC BER limit is 8.07 Gbit/s at the BER of 1.7×10^{-3} . We also measured the SNRs of Data 1 and Data 2 and their average SNRs were 10.96 dB and 14.45 dB, respectively.

Author Contributions: Data curation, W.-H.G.; funding acquisition, C.-W.C.; investigation, W.-H.G.; resources, Y.-H.C.; writing—original draft, W.-H.G.; writing—review & editing, Y.L., C.-W.C. and C.-H.Y. All authors have read and agreed to the published version of the manuscript.

Funding: This paper was supported by Ministry of Science and Technology, Taiwan, under Grant MOST-110-2221-E-A49-057-MY3, MOST-109-2221-E-009-155-MY3.

Institutional Review Board Statement: Not applicable.

Informed Consent Statement: Not applicable.

Data Availability Statement: The data presented in this study are available from the first author upon request.

Conflicts of Interest: The authors declare no conflict of interest.

References

1. Chow, C.W.; Yeh, C.H.; Liu, Y.; Lai, Y.; Wei, L.Y.; Hsu, C.W.; Chen, G.H.; Liao, X.L.; Lin, K.H. Enabling techniques for optical wireless communication systems. In Proceedings of the Optical Fiber Communication Conference 2020, San Diego, CA, USA, 8–12 March 2020. M2F.1.
2. Elgala, H.; Mesleh, R.; Haas, H. Indoor optical wireless communication: Potential and state-of-the-art. *IEEE Commun. Mag.* **2011**, *49*, 56–62. [\[CrossRef\]](#)
3. Lu, H.H.; Lin, Y.P.; Wu, P.Y.; Chen, C.Y.; Chen, M.C.; Jhang, T.W. A multiple-input-multiple-output visible light communication system based on VCSELs and spatial light modulators. *Opt. Exp.* **2014**, *22*, 3468–3474. [\[CrossRef\]](#)
4. Yu, T.C.; Huang, W.T.; Lee, W.B.; Chow, C.W.; Chang, S.W.; Kuo, H.C. Visible light communication system technology review: Devices, architectures, and applications. *Crystals* **2021**, *11*, 1098. [\[CrossRef\]](#)
5. Chi, N.; Zhou, Y.; Wei, Y.; Hu, F. Visible light communication in 6G: Advances, challenges, and prospects. *IEEE Vehicular Technol. Mag.* **2020**, *15*, 93–102. [\[CrossRef\]](#)
6. Luo, P.; Ghassemlooy, Z.; Minh, H.L.; Tang, X.; Tsai, H.M. Undersampled phase shift on-off keying for camera communication. In Proceedings of the WCSP'14, Hefei, China, 23–25 October 2014.
7. Wu, Y.C.; Chow, C.W.; Liu, Y.; Lin, Y.S.; Hong, C.Y.; Lin, D.C.; Song, S.H.; Yeh, C.H. Received-signal-strength (RSS) based 3D visible-light-positioning (VLP) system using kernel ridge regression machine learning algorithm with sigmoid function data preprocessing method. *IEEE Access* **2020**, *8*, 214269–214281. [\[CrossRef\]](#)
8. Lin, D.C.; Chow, C.W.; Peng, C.W.; Hung, T.Y.; Chang, Y.H.; Song, S.H.; Lin, Y.S.; Liu, Y.; Lin, K.H. Positioning unit cell model duplication with residual concatenation neural network (RCNN) and transfer learning for visible light positioning (VLP). *J. Lightw. Technol.* **2021**, *39*, 6366–6372. [\[CrossRef\]](#)
9. Shen, C.; Guo, Y.; Oubei, H.M.; Ng, T.K.; Liu, G.; Park, K.H.; Ho, K.T.; Alouini, M.S.; Ooi, B.O. 20-meter underwater wireless optical communication link with 1.5 Gbps data rate. *Opt. Express* **2016**, *24*, 25502–25509. [\[CrossRef\]](#) [\[PubMed\]](#)
10. Danakis, C.; Afgani, M.; Povey, G.; Underwood, I.; Haas, H. Using a CMOS camera sensor for visible light communication. In Proceedings of the OWC'12, Anaheim, CA, USA; pp. 1244–1248.
11. Lin, Y.S.; Chow, C.W.; Liu, Y.; Chang, Y.H.; Lin, K.H.; Wang, Y.C.; Chen, Y.Y. PAM4 rolling-shutter demodulation using a pixel-per-symbol labeling neural network for optical camera communications. *Opt. Express* **2021**, *29*, 31680–31688. [\[CrossRef\]](#) [\[PubMed\]](#)
12. Haas, H.; Yin, L.; Wang, Y.; Chen, C. What is LiFi? *J. Lightw. Technol.* **2016**, *34*, 1533–1544. [\[CrossRef\]](#)
13. Chow, C.W.; Yeh, C.H.; Liu, Y.F.; Liu, Y. Improved modulation speed of LED visible light communication system integrated to main electricity network. *Elect. Lett.* **2011**, *47*, 867–868. [\[CrossRef\]](#)
14. Minh, H.L.; O'Brien, D.; Faulkner, G.; Zeng, L.; Lee, K.; Jung, D.; Oh, Y.J.; Won, E.T. 100-Mb/s NRZ visible light communications using a postequalized white LED. *IEEE Photon. Technol. Lett.* **2009**, *21*, 1063–1065. [\[CrossRef\]](#)
15. Hsu, C.W.; Chow, C.W.; Lu, I.C.; Liu, Y.L.; Yeh, C.H.; Liu, Y. High speed imaging 3×3 MIMO phosphor white-light LED based visible light communication system. *IEEE Photon. J.* **2016**, *8*, 7907406. [\[CrossRef\]](#)
16. Cossu, G.; Khalid, A.M.; Choudhury, P.; Corsini, R.; Ciaramella, E. 3.4 Gbit/s visible optical wireless transmission based on RGB LED. *Opt. Exp.* **2012**, *20*, B501–B506. [\[CrossRef\]](#) [\[PubMed\]](#)
17. Chi, N.; Zhang, M.; Zhou, Y.; Zhao, J. 3.375-Gb/s RGB-LED based WDM visible light communication system employing PAM-8 modulation with phase shifted Manchester coding. *Opt. Exp.* **2016**, *24*, 21663–21673. [\[CrossRef\]](#) [\[PubMed\]](#)
18. James Singh, K.; Huang, Y.M.; Ahmed, T.; Liu, A.C.; Huang Chen, S.W.; Liou, F.J.; Wu, T.; Lin, C.C.; Chow, C.W.; Lin, G.R.; et al. Micro-LED as a promising candidate for high-speed visible light communication. *Appl. Sci.* **2020**, *10*, 7384. [\[CrossRef\]](#)
19. Tsonev, D.; Chun, H.; Rajbhandari, S.; McKendry, J.J.D.; Videv, S.; Gu, E.; Haji, M.; Watson, S.; Kelly, A.E.; Faulkner, G.; et al. A 3-Gb/s single-LED OFDM-based wireless VLC link using a gallium nitride μ LED. *IEEE Photon. Technol. Lett.* **2014**, *26*, 637–640. [\[CrossRef\]](#)
20. Lan, H.Y.; Tseng, I.C.; Lin, Y.H.; Lin, G.R.; Huang, D.W.; Wu, C.H. High-speed integrated micro-LED array for visible light communication. *Opt. Lett.* **2020**, *45*, 2203–2206. [\[CrossRef\]](#)
21. Chang, Y.H.; Huang, Y.M.; Gunawan, W.H.; Chang, G.H.; Liou, F.J.; Chow, C.W.; Kuo, H.C.; Liu, Y.; Yeh, C.H. 4.343-Gbit/s green semipolar (20–21)–LED for high speed visible light communication. *IEEE Photon. J.* **2021**, *13*, 7300204. [\[CrossRef\]](#)
22. Denault, K.A.; Cantore, M.; Nakamura, S.; DenBaars, S.P.; Seshadri, R. Efficient and stable laser-driven white lighting. *AIP Adv.* **2013**, *3*, 072107. [\[CrossRef\]](#)
23. Chi, Y.C.; Hsieh, D.H.; Lin, C.Y.; Chen, H.Y.; Huang, C.Y.; He, J.H.; Ooi, B.; DenBaars, S.P.; Nakamura, S.; Kuo, H.C.; et al. Phosphorous diffuser diverged blue laser diode for indoor lighting and communication. *Sci. Rep.* **2015**, *5*, 1–9. [\[CrossRef\]](#)
24. Chang, C.H.; Li, C.Y.; Lu, H.H.; Lin, C.Y.; Chen, J.H.; Wan, Z.W.; Cheng, C.J. A 100-Gb/s multiple-input multiple-output visible laser light communication system. *J. Lightw. Technol.* **2014**, *32*, 4723–4729. [\[CrossRef\]](#)
25. Liu, X.; Yi, S.; Zhou, X.; Fang, Z.; Qiu, Z.J.; Hu, L.; Cong, C.; Zheng, L.; Liu, R.; Tian, P. 34.5 m underwater optical wireless communication with 2.70 Gbps data rate based on a green laser diode with NRZ-OOK modulation. *Opt. Express* **2017**, *25*, 27937–27947. [\[CrossRef\]](#)
26. Wei, L.Y.; Chen, S.I.; Yeh, C.H.; Liu, Y.; Chen, G.H.; Peng, C.W.; Gunawan, W.H.; Chang, Y.H.; Guo, P.C.; Chow, C.W. 2.333-Tbit/s bi-directional optical mobile networks using optical wireless communication (OWC). *Opt. Comm.* **2020**, *475*, 126187. [\[CrossRef\]](#)

-
27. Wei, L.Y.; Liu, Y.; Chow, C.W.; Chen, G.H.; Peng, C.W.; Guo, P.C.; Tsai, J.F.; Yeh, C.H. 6.915-Gbit/s white-light phosphor laser diode-based DCO-OFDM visible light communication (VLC) system with functional transmission distance. *Electron. Lett.* **2020**, *56*, 945–947. [[CrossRef](#)]
 28. Wu, T.C.; Chi, Y.C.; Wang, H.Y.; Tsai, C.T.; Huang, Y.F.; Lin, G.R. Tricolor R/G/B laser diode based eye-safe white lighting communication beyond 8 Gbit/s. *Sci. Rep.* **2017**, *7*, 11. [[CrossRef](#)]
 29. Wei, L.Y.; Chow, C.W.; Chen, G.H.; Liu, Y.; Yeh, C.H.; Hsu, C.W. Tricolor visible-light laser diodes based visible light communication operated at 40.665 Gbit/s and 2 m free-space transmission. *Opt. Exp.* **2019**, *27*, 25072–25077. [[CrossRef](#)] [[PubMed](#)]
 30. Gunawan, W.H.; Liu, Y.; Chow, C.W.; Chang, Y.H.; Peng, C.W.; Yeh, C.H. Two-level laser diode color-shift-keying orthogonal-frequency-division-multiplexing (LD-CSK-OFDM) for optical wireless communications (OWC). *J. Lightwave Technol.* **2021**, *39*, 3088–3094. [[CrossRef](#)]
 31. Yeh, C.H.; Chen, H.Y.; Chow, C.W.; Liu, Y.L. Utilization of multi-band OFDM modulation to increase traffic rate of phosphor-LED wireless VLC. *Opt. Exp.* **2015**, *23*, 1133–1138. [[CrossRef](#)] [[PubMed](#)]
 32. Saito, Y.; Kishiyama, Y.; Benjebbour, A.; Nakamura, T.; Li, A.; Higuchi, K. Non-orthogonal multiple access (NOMA) for cellular future radio access. In Proceedings of the VTC Spring 2013, Dresden, Germany, 2–5 June 2013; pp. 1–5.
 33. Wu, Q.; Feng, Z.; Tang, M.; Li, X.; Luo, M.; Zhou, H.; Fu, S.; Liu, D. Digital domain power division multiplexed dual polarization coherent optical OFDM transmission. *Sci. Rep.* **2018**, *8*, 15827. [[CrossRef](#)] [[PubMed](#)]
 34. Adnan, A.; Liu, Y.; Chow, C.W.; Yeh, C.H. Analysis of non-Hermitian symmetry (NHS) IFFT/FFT size efficient OFDM for multiple-client non-orthogonal multiple access (NOMA) visible light communication (VLC) system. *Opt. Comm.* **2020**, *472*, 125991. [[CrossRef](#)]